Applying watershed outlet sediment geochemistry pattern to indicate long-term agricultural non-point source (NPS) pollution loading

Wei Ouyang[a]*, Wei Jiao[a], Xiaoming Li[a], Elisa Giubilato[b], Andrea Critto[b]

[a] *State Key Laboratory of Water Environment Simulation, School of Environment, Beijing Normal University, Beijing 100875, China*
[b] *Department of Environmental Sciences, Informatics and Statistics, Ca' Foscari University of Venice, Venice 30123, Italy*

ABSTRACT

Agricultural non-point source (NPS) pollution cause more risk to the water safety and some part of loading can be accumulated in the watershed outlet section. It was hypothesized that the geochemistry characteristics of watershed outlet sediment can present the long-term NPS pollution loading. It is crucial for evaluating the historical interactions between sediment properties with watershed NPS loading. In this study, we collected the sediment core from the outlet of a typical agricultural watershed in Northeast China. The core was age dated by ^{210}Pb method, and sedimentation rates were determined using the constant rate of supply model. It was found that total nitrogen (TN), total phosphorus (TP), Cd, Pb, Cu, Ni and Cr accumulations in the sediments generally showed a trend of fluctuating increase with the highest sedimentation fluxes all observed around 1998. The measurement of specific mass sedimentation rates reflected watershed soil erosion dynamics during long-term agricultural development, which was closely associated with the sediment geochemistry. However, the excessive application of phosphorus fertilizers was identified as the major cause for recent sediment geochemistry variability. With Soil and Water Assessment Tool, the historical interactions of sediment properties with agricultural NPS pollution were further evaluated. To some extent, the N leaching process weakened this interaction, but the historical accumulation of TP and heavy metals in sediments generally correlated well with watershed NPS TP loading. The regression analysis suggested that Pb and Cr were the most suitable indexes to assess the long-term NPS TN and TP pollution, respectively.

Keywords: Agricultural NPS pollution; Sediment core; ^{210}Pb dating; SWAT; Watershed water quality

1. Introduction

Sedimentation processes usually occur during the subsequent transport of various pollutants into surface water (Ramalhosa et al., 2006). Consequently, the sediment geochemistry is considered as a useful indicator for

*Corresponding author. Tel.: +86 10 58804585; fax: +86 10 58804585. *E-mail address:* wei@itc.nl (W. Ouyang).

environmental changes and anthropogenic impacts (Chatterjee et al., 2007; Nath et al., 2000). It has been widely recognized that intensive agricultural development can cause watershed water pressures via soil erosion and the release of associated non-point source (NPS) pollutants, such as nitrogen, phosphorus and heavy metals (Jain, 2002; Jiao et al., 2014). Parts of NPS nitrogen (N) and phosphorus (P) discharge by the upland process with water and accumulate in the river sediment. It is hypothesized that the vertical sediment geochemistry characteristics have correlation with the NPS loading history. However, research regarding the sediment property responses to long-term agricultural NPS pollution remains scarce.

Over the past few decades, the study of sediment cores has shown to be an excellent approach for establishing the effects of anthropogenic and natural processes on sedimentary environments (Shotyk, 2002). Vertical profiles of pollutant species in the sediment cores are commonly used as ‘‘historical pollution records’’ of whole watershed (Harikumar and Nasir, 2010). In order to inverse identify the pollution history, it is essential to estimate the sedimentation rates and sediment ages. The results can also give valuable information on the soil erosion dynamics of a watershed (Mabit et al., 2014), which is an important aspect in relation to agricultural NPS pollution. In this context, application of radiometric methods to sedimentary chronology has developed rapidly and enjoyed considerable success (Saravana Kumara et al., 1999; Du and Walling, 2012). In particular, the half-life of ^{210}Pb (22.3 years) makes it an ideal radioisotope for dating sediments from the past 100-150 years. To date, this method has been used extensively in different sedimentary environments, including wetlands, lakes, reservoirs, flood plains, estuaries and coastal marines (Mabit et al., 2014).

Effective reduction of NPS pollution in agricultural watersheds is widely required as the higher standard for the watershed water management (Shen et al., 2015). Consequently, the studies seeking a better understanding of agricultural watershed management have expressed increasing concern over the quantification of NPS pollution loadings (Dechmi and Skhiri, 2013; Heathwaite et al., 2005). For this purpose, a number of water quality models at watershed scale have been developed and applied. Among these models, the Soil and Water Assessment Tool (SWAT) is frequently used to assess the NPS nitrogen and phosphorus pollution over long timescales in large agricultural watersheds (Laurent and Ruelland, 2011; Ouyang et al., 2010). However, it should be noted that the modeling methods are usually quite time consuming, because they need to collect many input data for model parameters (Choi and Blood, 1999). Applying sediment geochemistry to indicate the agricultural NPS pollution is a potential way to achieve the knowledge needed to support routinely management, especially in data-sparse or un-gauged watershed (Jiao et al., 2014).

The river sediment analysis is the widely accepted indicator for watershed environmental quality (Smith, 2001). Based on the hypothesis of the interaction between sediment and NPS pollution loading, we presented a new approach to ensure that the sediment geochemistry indicators can function properly on a long-time scale. The interaction principle was achieved by the integration of SWAT modeling and ^{210}Pb-dated sediment analysis. The primary objectives of this study were: (1) to analyze and date the total nitrogen (TN), total phosphorus (TP), Cd, Pb, Cu, Ni and Cr accumulations in sediment at watershed outlet; (2); to identify the long-term NPS nitrogen and phosphorus loading under agricultural development and (3) to evaluate the historical interactions of these sediment properties with watershed NPS TN and TP pollution, thus selecting the most proper indication indexes.

2. Materials and methods

2.1. Study area description

The study area is located in Sanjiang Plain, Northeast China, which has a total watershed area of 24,863 km^2 (Fig. 1). Along with intensive regional agricultural development, the agriculture is the only economy in this watershed since 1950s. Consequently, about half of natural wetlands, forests and grasslands were reclaimed into paddy lands and uplands, where rice and maize are the two main types of crops being cultivated. This watershed has a frigid temperate, continental monsoon climate with the average annual temperature of 1.91 ◦C. The mean annual precipitation is approximately 600 mm, most of which falls between May and September (Ouyang et al., 2014). The local rivers, characterized by a seasonal hydrological regime, generally flow southwest to northeast.

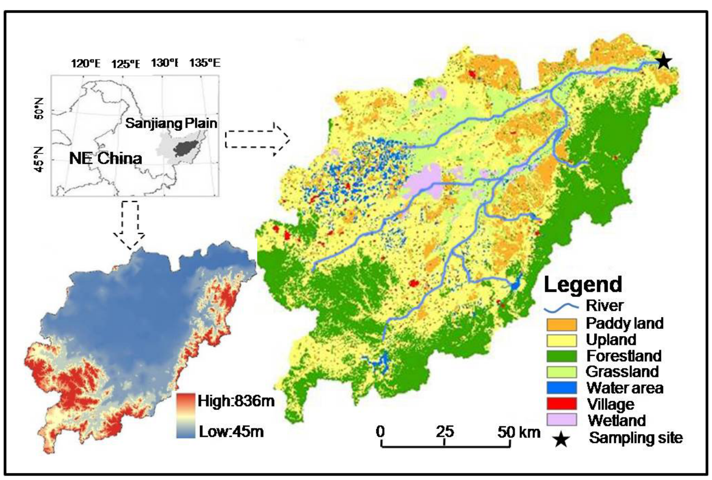

Fig. 1 Location of the study area showing topography, land uses and sampling site

2.2. Watershed outlet sediment coring and pretreatment

In July 2013, one river sediment core of 40 cm in length was collected from the watershed outlet (Fig. 1). During the coring, special care was taken to ensure minimum disturbance of the sediment-water interface. The gravity-coring unit was therefore lowered as slowly as possible into the sediment to avoid lateral movements, which would be caused by the pressure wave created by the descent of the corer. After collection, the sediment core was sliced at 1 cm intervals down to the bottom. All the sliced layers were sealed in polyethylene bags and transported to the laboratory immediately, where they were air dried at room temperature, ground with a pestle and mortar and passed through a 100-mesh nylon sieve.

2.3. ^{210}Pb activities and sedimentation rates determination

The chronology of the sediment core was determined by ^{210}Pb method using high-resolution gamma ray spectrometry with an HPGe detector. There are two sources for ^{210}Pb found in sediments: one comes from the in situ decay of ^{226}Ra and it is called supported ($^{210}Pb_{sup}$); and the second source derives from natural fallout (Krishnaswamy et al., 1971). In consequence, the total activity of this isotope ($^{210}Pb_{tot}$) in sediments is the sum of supported ($^{210}Pb_{sup}$) and atmospherically derived ^{210}Pb. The latter term, called unsupported or excess ($^{210}Pb_{ex}$), can be obtained by subtracting the measured activity in secular equilibrium with ^{226}Ra from the $^{210}Pb_{tot}$ for each sediment sample (San Miguel et al., 2004). After a month of storage in sealed containers to allow radioactive equilibration, $^{210}Pb_{tot}$ was determined from the 46.5-keV gamma ray emission and ^{226}Ra from the 295.2-keV and 351.9-keV gamma rays emitted by its daughter isotope ^{214}Pb. The precision of this analytical method was usually higher than 10% (Xia et al., 2011). To help date the sediment core, sedimentation rates were estimated by the constant rate supply (CRS) model, which assumes a constant rate of $^{210}Pb_{ex}$ from atmospheric fallout but allows sediment accumulation to vary (Appleby and Oldfield, 1978).

2.4. Sediment total nitrogen, phosphorus and heavy metal concentrations analysis

In order to identify the sediment geochemistry variability under long-term agricultural development, we analyzed the total nitrogen (TN), total phosphorus (TP), Cd, Pb, Cu, Ni and Cr concentrations for each sediment sample. The TN was measured directly by a CHN Elemental Analyzer. For the analysis of TP and heavy metal concentrations, sediment samples were digested with an acid mixture of HF-HNO_3-$HClO_4$ and measured using the inductively coupled plasma-atomic emission spectroscopy (ICP-AES). The analytical data quality was assessed by measuring simultaneously the reference material GBW-07401, which showed that the average recoveries generally ranged from 97.47 to 104.14%.

2.5. Watershed NPS total nitrogen and phosphorus loadings simulation

The SWAT model was also applied to estimate watershed NPS TN and TP loadings in the period 1977–2013. The NPS nitrogen (N) in the forms of organic and nitrate were simulated, and their sum represents the total N

(TN). The NPS phosphorus (P) was modeled in the forms of organic, soluble and sediment contributions, and their sum represents the total P (TP). To run the model, SWAT databases were firstly prepared and imported, including topography (1:250 000), the four-year land covers (1:1 000 000), the climate information, and the soil properties (1:1 000 000) (Fig. 1). The watershed climatic features were simulated with the daily historical monitoring data (minimum and maximum temperature, wind speed, precipitation and solar radiation) obtained from three weather stations between 1973 and 2013. The local agricultural management information was added to improve the modeling efficiency. After field investigations, local agricultural practices of paddy rice and maize were also taken into account to improve the modeling efficiency (Ouyang et al., 2013).

After the sensitivity analysis, the SWAT model was calibrated with monitoring data obtained in the first twenty-four months and later validated with data from an additional two years. The model was validated in the order of streamflow, soil erosion and nutrient pollution loads with the SWAT-CUP system (Fig. 2). With the routing monitoring data of streamflow and sand concentration, and the sixteen dominant parameters that affected these two indicators were validated (Fig. 3). The modeling performances of the streamflow and sediment were evaluated using the coefficient of determination (R^2) and the Nash-Sutcliffe efficiency (E_{NS}), which was bigger than 0.698. The details of SWAT applicability to this watershed can be obtained from our earlier paper (Ouyang et al., 2014).

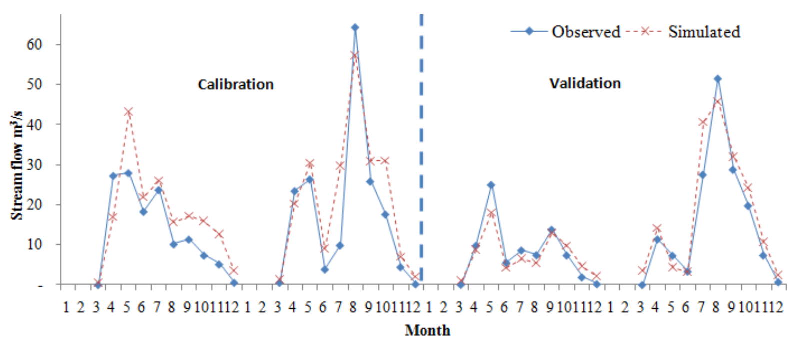

Fig. 2 Calibration and validation of the streamflow

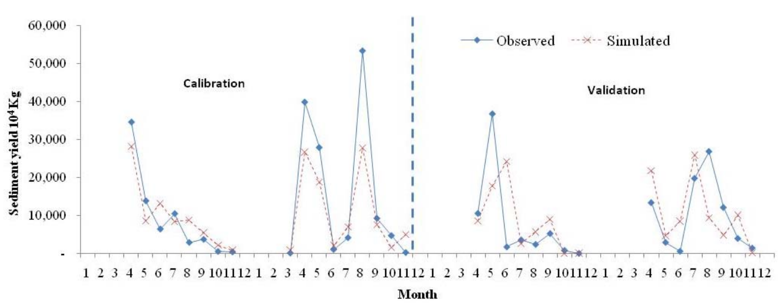

Fig. 3 Calibration and validation of the sand concentration

2.6. Sedimentation flux calculation and regression analysis

The concept of "sedimentation flux" considers possible sediment changes over time. In this study the TN, TP, Cd, Pb, Cu, Ni and Cr fluxes to the sediment core were calculated by multiplying their concentrations and the CRS modeled mass sedimentation rate for each layer (Alvarez-Iglesias et al., 2007). As the remote sensing data availability, the yearly watershed NPS TN and TP loadings were simulated from 1977–2013. In order to calculate the regression between the NPS loading with sedimentation flux, the sedimentation dates in the period of 1977–2013 were selected. So, the sedimentation dates of 2013, 2008, 2003, 1998, 1993, 1988, 1983 and 1978 were identified in this period as the regression analysis years.

3. Results

3.1. Watershed outlet sedimentation rates and age dating

The total, supported and excess ^{210}Pb activities, as well as CRS modeled sedimentation rates are shown in Table 1 as a function of sediment depth. In general, the $^{210}Pb_{tot}$ activities varied significantly from 16.97 to 28.64 Bg/kg, with an average activity of 21.41 Bg/kg. However, the $^{210}Pb_{sup}$ activities were relatively constant and ranged between 13.30 and 16.97 Bg/kg. The $^{210}Pb_{ex}$ activities were calculated as the difference between $^{210}Pb_{tot}$ and $^{210}Pb_{sup}$, which reached its maximum of 14.19 Bg/kg at the surface sediment. It was found that the $^{210}Pb_{ex}$ activities generally showed an almost monotonic decline with sediment depth. This decline indicated a rather undisturbed environment for the sediment core, where bioturbation or physical mixing could be considered negligible. According to CRS modeling results, the watershed mass sedimentation rates ranged from 45.86 to 523.15 mg/cm^2·a, with an average linear rate of 0.40 cm/a. Therefore, if the linear rate was maintained, the 40 cm sediment core actually spanned a time period from 1913 to 2013.

Table 1 Total, supported and excess ^{210}Pb activities, as well as CRS modeled sedimentation rates

Depth (cm)	$^{210}Pb_{tot}$ (Bg/kg)	$^{210}Pb_{sup}$ (Bg/kg)	$^{210}Pb_{ex}$ (Bg/kg)	Mass rate (mg/cm^2·a)	Linear rate (cm/a)	Sedimentation date (Year)
0-1	28.56	14.37	14.19	497.71	0.62	2013
1-2	28.64	14.89	13.75	488.18	0.60	
2-3	27.34	14.75	12.59	504.82	0.60	2008
3-4	26.38	13.95	12.43	484.76	0.55	
4-5	27.49	16.25	11.24	506.16	0.60	2003
5-6	25.68	15.01	10.67	504.71	0.58	
6-7	24.17	14.42	9.75	523.15	0.59	1998
7-8	24.30	14.72	9.58	504.16	0.59	
8-9	23.59	14.54	9.05	505.47	0.60	1993
9-10	21.70	13.31	8.39	516.41	0.61	
10-11	24.02	15.82	8.20	501.66	0.58	1988

11-12	21.21	13.69	7.52	519.00	0.61	
12-13	22.69	15.40	7.29	506.34	0.57	1983
13-14	21.52	14.12	7.40	472.15	0.53	
14-15	21.03	14.02	7.01	469.77	0.53	1978
15-16	23.21	16.43	6.78	453.36	0.48	
16-17	22.02	15.61	6.41	452.50	0.49	1973
17-18	22.71	16.41	6.30	430.03	0.45	
18-19	19.68	13.79	5.89	427.52	0.44	1968
19-20	20.29	15.11	5.18	449.13	0.47	
20-21	21.91	16.97	4.94	444.86	0.46	1963
21-22	21.04	16.13	4.91	419.44	0.42	
22-23	19.39	14.80	4.59	412.94	0.41	1958
23-24	20.50	16.31	4.19	415.20	0.42	
24-25	18.90	14.80	4.10	394.95	0.39	1953
25-26	20.12	16.11	4.01	373.68	0.36	
26-27	20.28	16.31	3.97	342.54	0.32	1948
27-28	18.58	14.78	3.80	319.59	0.31	
28-29	18.56	15.25	3.31	330.27	0.32	1943
29-30	18.97	15.56	3.41	293.08	0.26	
30-31	18.50	15.61	2.89	300.66	0.27	1938
31-32	19.00	16.21	2.79	278.04	0.25	
32-33	18.20	15.52	2.68	253.73	0.22	1933
33-34	19.18	16.68	2.50	236.66	0.20	
34-35	18.51	16.00	2.51	199.30	0.17	1928
35-36	18.80	16.58	2.22	184.01	0.16	
36-37	17.83	15.92	1.91	163.04	0.12	1923
37-38	16.97	14.97	2.00	124.56	0.09	
38-39	17.52	15.68	1.84	89.70	0.06	1918
39-40	17.43	15.62	1.81	45.86	0.04	

3.2. Total nitrogen and phosphorus accumulations in the sediment core

Considering that this watershed has begun to experience an extensive agricultural reclamation since the 1950s, the sedimentation fluxes of TN and TP in this period are presented in Fig. 4._During the long-term agricultural development, the watershed TN and TP accumulations in sediments generally showed a trend of fluctuating increase, with the highest sedimentation fluxes all observed around 1998. The TN fluxes ranged from 222.43 to 313.89 ug/cm^2·a, with an average of 280.17 ug/cm^2·a. The TP fluxes were generally low before 1988, but has exceeded TN fluxes since then with an average of 288.64 ug/cm^2·a. By comparison, the watershed TN sedimentation fluxes showed much weaker historical variability than TP fluxes, especially in the recent period.

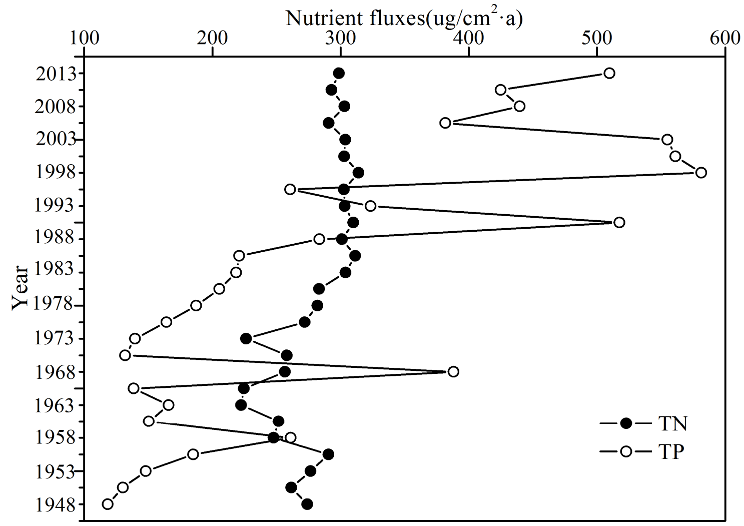

Fig. 4 Historical accumulation of total nitrogen and phosphorus in the sediment core

3.3. Heavy metal accumulations in the sediment core

Following the same flowchar, the Cd, Pb, Cu, Ni and Cr fluxes to the sediment core from 1948 to 2013 are also illustrated in Fig. 5. In general, the sedimentation fluxes of these heavy metals fluctuated with an increasing trend: Cd ranged from 0.04 to 0.16 ug/cm^2·a, with the average flux of 0.09 ug/cm^2·a; Pb ranged from 6.38 to 10.14 ug/cm^2·a, with the average flux of 8.31 ug/cm^2·a; Cu ranged from 6.70 to 11.50 ug/cm^2·a, with the average flux of 8.99 ug/cm^2·a; Ni ranged from 8.78 to 14.40 ug/cm^2·a, with the average flux of 11.87 ug/cm^2·a; and Cr ranged from 21.00 to 31.99 ug/cm^2·a, with the average flux of 25.26 ug/cm^2·a. For all heavy metals, the highest sedimentation fluxes also occurred in 1998, which implies that they may have a similar watershed release history with TN and TP.

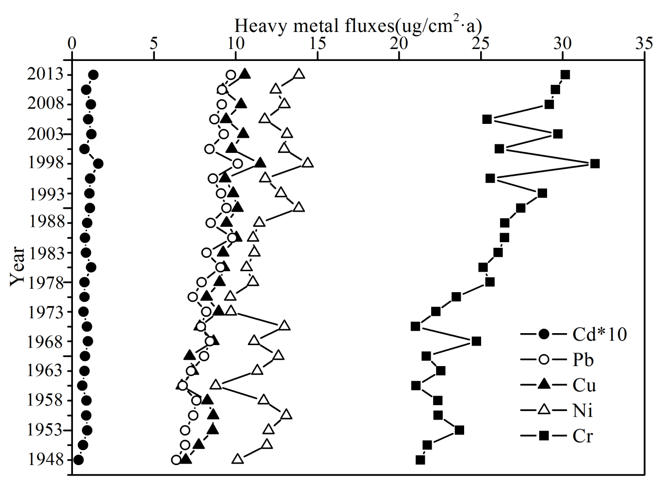

Fig. 5 Historical accumulation of heavy metals in the sediment core

3.4. Long-term watershed NPS total nitrogen and phosphorus loadings

With SWAT model, the watershed NPS TN and TP loadings were simulated in the period 1977–2013. As shown in Fig. 6, the watershed NPS nutrients pollution generally displayed strong variability in the total simulation period. The TN loadings ranged from 3.17 to 13.41 kg/ha, with the annual average of 7.92 kg/ha. The TP loadings ranged from 0.40 to 1.78 kg/ha, with the annual average of 0.95 kg/ha. The highest TN and TP loadings all occurred in 1998, which were 1.69 and 1.87 times larger than the simulated annual averages, respectively. These results were in agreement with the highest accumulation fluxes in 1998 at a sediment depth of 7 cm indicating the CRS modeled dates, at least in the upper part of the core, were reasonable.

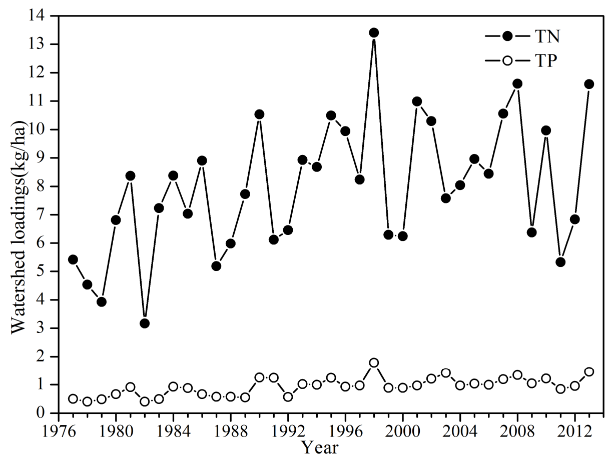

Fig. 6 Long-term watershed NPS total nitrogen and phosphorus loadings

3.5. Relationships of NPS nitrogen and phosphorus with sediment properties

After obtaining the long-term NPS TN and TP loadings, the regression analysis was applied to assess their relationships with TN, TP and heavy metals sedimentation fluxes in 2013, 2008, 2003, 1998, 1993, 1988, 1983 and 1978 (Fig. 7). It was found that the sedimentation flux of TN generally showed a positive relationship with watershed NPS loading, with the r^2 value of 0.464. However, the relationship was much weaker when compared to Cd, Pb, Cu, Ni and Cr. These results clearly implied that the accumulations of heavy metals in sediments were more sensitive to NPS pollution than that of TN. By comparison of the fitting lines, Pb had a higher r^2 value than those of other heavy metals. It can therefore be selected as the most proper sediment index to assess the long-term watershed NPS TN loading.

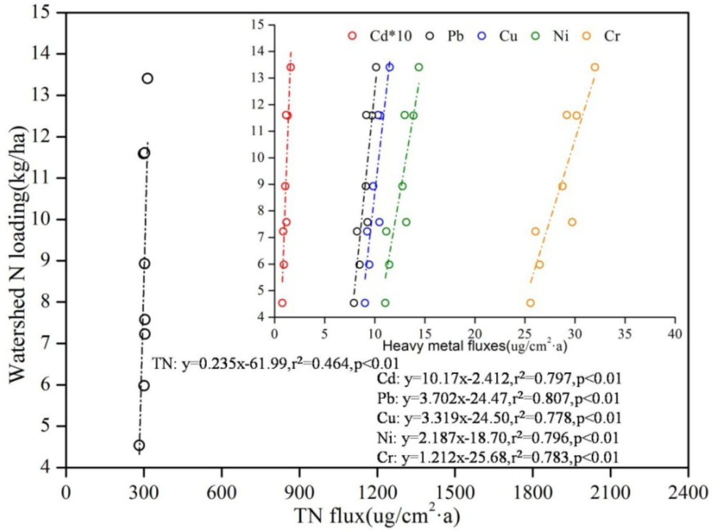

Fig. 7 Relationships between watershed NPS total nitrogen loading and sediment properties

The historical relationships of NPS TP loading with watershed sedimentation fluxes are shown in Fig. 8. Compared to watershed NPS nitrogen pollution, the sediment property responses to NPS phosphorus pollution were much stronger. In general, the TP sedimentation flux correlated well with NPS loading with the r^2 value of 0.943. However, this value was still lower than those for Cu, Ni and Cr. Among these heavy metals, Cr was found to provide more reliable information for indicating the watershed NPS TP pollution.

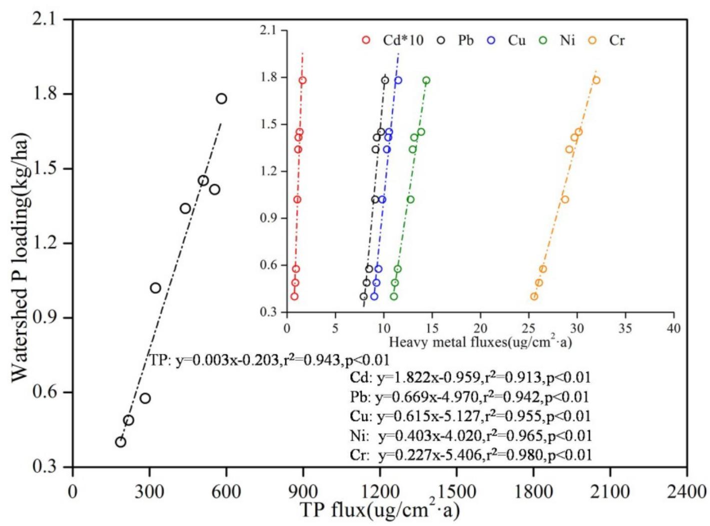

Fig. 8 Relationships between watershed NPS total phosphorus loading and sediment properties (Y)

4. Discussion

4.1. Watershed outlet sediment geochemistry variability with long-term agricultural development

The intensive agricultural activities impact the ecological environment quality and also affect the watershed water quality (Hosono et al., 2007). One of the most significant impacts is from the increased NPS pollutant loadings, which has caused serious water pollution problems in recent decades (Zia et al., 2013). In this study, the impact of long-term agricultural development on watershed water environment was adequately evaluated by analyzing one river sediment core at watershed outlet. The watershed TN, TP and heavy metals accumulations in sediments generally showed a trend of fluctuating increase during the long-term agricultural development (Fig. 4 and Fig. 5). Such sediment geochemistry variability is in agreement with the cases in other watersheds of China, suggesting a continuously growing water environment pressure (Tang et al., 2010; Wang et al., 2004).

It is wildly accepted that the frequent agricultural activities can accelerate soil erosion, which therefore has a close relationship with watershed sediment geochemistry (Quinton and Catt, 2007). In general, the measurements of specific mass sedimentation rates reflect a historical record of watershed soil erosion processes. According to CRS modeled results, the study watershed had an average sedimentation rate of 472.18 $mg/cm^2\cdot$during the period 1953-2013 (Table 1). The rate is much higher in later period than those in the earlier years and therefore highlights the long-term cultivation impact. However, it can be seen that the abrupt change in mass sedimentation rate, as well as TN, TP and heavy metal fluxes all occurred around 1998. This should be attributed to an extreme flood in this year, because the watershed soil erosion dynamics are also determined by natural hydrology and could vary greatly from year to year (Oeurng et al., 2010). By comparison, the sedimentation rates are almost constant after 2008, but the sedimentation fluxes of TP and heavy metals generally still exhibit an obvious increasing trend. With more concerns about environmental protection, some soil and water conservation measurements have gradually been implemented in recent years. However, the amount of phosphate fertilizer usage has increased significantly to obtain higher crop yields, reaching 87 kg P/ha by 2010 (Jiao et al., 2014). Therefore, the excessive application of phosphorus fertilizers that contain a variety of trace metals as impurities may be the major cause for recent sediment geochemistry variability.

4.2. Historical interactions of sediment properties with long term NPS pollution loading

In order to evaluate the historical interactions of sediment properties with NPS pollution, the watershed NPS TN and TP loadings were simulated by SWAT in the period 1977-2013 (Fig. 6). In general, the watershed NPS pollutions display a strong temporal variability in the whole simulation period. However, it is noticeable that the TN fluxes in sediments remained relatively stable in recent times, which is disagreed with the simulation results. A proper explanation for this is that leaching has occurred after nitrogen deposition in sediments, and the NPS nitrogen pollution forms mainly in soluble form (Almasri and Kaluarachchi, 2007). Conversely, the accumulations of heavy metals in sediments are found to be more sensitive to watershed NPS pollution than TN accumulation. By comparison of the fitting lines, Pb had a higher R^2 value than those of TN and other heavy metals. Therefore, it is selected as the most proper sediment index to indicate the long-term NPS TN pollution.

When compared to watershed NPS TN pollution, the NPS TP loading was always found to be much lower in the total simulation period. However, previous study indicate that even slight changes of NPS phosphorus pollution can also greatly affect water quality in highly agricultural watershed (Tesoriero et al., 2009). By comparison, the TP fluxes exhibited stronger variability in sediments and they exceeded TN fluxes since around 1988 (Fig. 6). Because the formation and transport of NPS phosphorus occurs mainly in particulate form (Leone et al., 2008), the historical accumulation of TP in sediments generally correlated well with watershed NPS loading with r^2 value of 0.943. However, this value is still lower than those for some heavy metals such as Cu, Ni and Cr. Among these heavy metals, Cr is considered as a major pollutant in phosphorus fertilizers (Ouyang et al., 2012), which thus can provide more reliable information for assessing the NPS TP pollution.

4.3. Implications for watershed NPS nitrogen and phosphorus control

With continuous industrial emissions control, the agricultural NPS has been increasingly recognized as a major contributor of watershed nitrogen and phosphorus pollution (Dupas et al., 2015). Consequently, the assessment of agricultural NPS loading is becoming more important when formulating effective watershed water management strategies (Rao et al., 2009). In this research, the interactions analysis proved the hypotheses between the sediment geochemistry with history NPS pollution loading. The approach we demonstrated that it is feasible to utilize the overall sediment geochemistry information to assess the long-term NPS TN and TP pollution before applying the complicated modeling. However, it must be noted that this approach seemed to be more applicable in indicating watershed NPS phosphorus pollution.

To some extent, the leaching process weakened the historical interactions of sediment properties with watershed NPS TN loading. Therefore, some attentions should be paid to the watershed groundwater pollution when implementing effective NPS nitrogen control. In an agricultural watershed, soil heavy metals tend to enter water environment together with various nutrients pollution (Yang et al., 2013). Since heavy metals deposited in sediments are not biodegradable, it is better for tracing the watershed nitrogen and phosphorus pollution in terms of heavy metals than by using nutrient indexes alone (Jin et al., 2010). The regression analyses suggest that Pb and Cr are the most suitable indexes to assess the long-term NPS TN and TP pollution, respectively.

5. Conclusions

This study proved the hypothesis that the watershed agricultural NPS pollution loading had close correlation with watershed outlet sediment geochemistry patterns. This approach can be used to indicate the long-term NPS pollution. With SWAT model, the historical interactions of sediment properties with NPS TN and TP pollution were further evaluated. The historical accumulations of TP and heavy metals in sediments generally correlated well with watershed NPS TP loading. The regression analysis suggested that Pb and Cr were the most suitable indexes to assess the long-term NPS TN and TP pollution, respectively. In general, the annual assessment results are more reasonable.

By analyzing the river sediment core at watershed out, it was found that the watershed TN, TP, Cd, Pb, Cu, Ni and Cr accumulations in sediments showed a trend of fluctuating increase. According to CRS modeled results, the watershed had an average mass sedimentation rate of 472.18 $mg/cm^2 \cdot a$ in the period 1953-2013. This value was much higher than those in the years before 1953, which highlighted the long-term cultivation impact on NPS pollution loading since 1950s. However, the abrupt change in mass sedimentation rate, as well as TN, TP and heavy metal fluxes all occurred around 1998, which should be attributed to an extreme flood in this year. By comparison, the watershed sedimentation rates were almost constant after 2008, but the sedimentation fluxes of TP and heavy metals generally still exhibited an obvious increasing trend. The excessive application of phosphorus fertilizers that contain a variety of trace metals as impurities, maybe the major cause for recent sediment geochemistry variability.

Acknowledgements

This work was financially supported by the National Natural Science Foundation of China (Grant Nos. 41371018, 41271463), the Supporting Program of the "Twelfth Five-year Plan" for Science & Technology Research of China (2012BAD15B05), and the European Union Seventh Framework Programme (FP7/2007-2013) under Grant Agreement No. 269233–GLOCOM (Global Partners in Contaminated Land Management).

References

Almasri, M.N., Kaluarachchi, J.J., 2007. Modeling nitrate contamination of groundwater in agricultural watersheds. Journal of Hydrology, 343, 211-229.
Appleby, P.G., Oldfield, F., 1978. The calculation of lead-210 dates assuming a constant rate of supply of unsupported Pb-210 in the sediment. Catena, 5, 1-8.
Chatterjee, M., Silva Filho, E.V., Sarkar, S.K., Sella, S.M., Bhattacharya, A., Satpathy, K.K., Prasad, M.V.R.,

Chakraborty, S., Bhattacharya, B.D., 2007. Distribution and possible source of trace elements in the sediment cores of a tropical macrotidal estuary and their ecotoxicological significance. Environment International, 33, 346-356.

Choi, K.S., Blood, E., 1999. Modeling developed coastal watersheds with the agricultural non-point source model. Journal of the American Water Resources Association, 35, 233-44.

Dechmi, F., Skhiri, A., 2013. Evaluation of best management practices under intensive irrigation using SWAT model. Agricultural Water Management, 123, 55-64.

Dupas, R., Delmas, M., Dorioz, J.M., Garnier, J., Moatar, F., Gascuel-Odoux, C., 2015. Assessing the impact of agricultural pressures on N and P loads and eutrophication risk. Ecological Indicators, 48, 396-407.

Harikumar, P.S., Nasir, U.P., 2010. Ecotoxicological impact assessment of heavy metals in core sediments of a tropical estuary. Ecotoxicology and Environmental Safety, 73, 1742-1747.

Heathwaite, A.L., Dils, R.M., Liu, S., Carvalho, L., Brazier, R.E., Pope, L., Hughes, M., Philips, G., May, L., 2005. A tiered risk-based approach for predicting diffuse and point source phosphorus losses in agricultural areas. Science of the Total Environment, 344, 225-239.

Hosono, T., Nakano, T., Igeta, A., Tayasu, I., Tanaka, T., Yachi, S., 2007. Impact of fertilizer on a small watershed of Lake Biwa: Use of sulfur and strontium isotopes in environmental diagnosis. Science of the Total Environment, 384, 342-354.

Jain, C.K., 2002. A hydro-chemical study of a mountainous watershed: the Ganga, India. Water Research, 39, 1262-1274.

Jiao, W., Ouyang, W., Hao, F.H., Huang, H.B., Shan, Y.S., Geng, X.J., 2014. Combine the soil water assessment tool (SWAT) with sediment geochemistry to evaluate diffuse heavy metal loadings at watershed scale. Journal of Hazardous Materials, 280, 252-259.

Jin, Z.D., Cheng, H.X., Chen, L., Li, X.D., Zhu, G.W., Zhuang, G.M., Qian, N., 2010. Concentrations and contamination trends of heavy metals in the sediment cores of Taihu Lake, East China, and their relationship with historical eutrophication. Chinese Journal of Geochemistry, 29, 33-41.

Krishnaswamy, S., Lal, D., Martin, J.M., Meybeck, M., 1971. Geochronology of lake sediments. Earth and Planetary Science Letters, 11, 407-414.

Laurent, F., Ruelland, D., 2011. Assessing impacts of alternative land use and agricultural practices on nitrate pollution at the catchment scale. Journal of Hydrology, 409, 440-450.

Leone, A., Ripa, M.N., Boccia, L., Lo Porto, A., 2008. Phosphorus export from agricultural land: a simple approach. Biosystems Engineering, 101, 270-280.

Mabit, L., Benmansour, M., Abril, J.M., Walling, D.E., Meusburger, K., Iurian, A.R., Bernard, C., Tarjan, S., Owens, P.N., Blake, W.H., Alewell, C., 2014. Fallout ^{210}Pb as a soil and sediment tracer in catchment sediment budget investigations: A review. Earth-Science Reviews, 138, 335-351.

Nath, B.N., Kuzendory, H., Pluger, W.L., 2000. Influence of provenancer weathering and sedimentary process on the elemental ratios of the fine-grained fractions of the bed load sediments from Vembanad Lake and the adjoining continental shelf, south west coast of India. Journal of Sedimentary Petrology, 70, 1081-1094.

Oeurng, C., Sauvage, S., Sanchez-Perez, J.M., 2010. Dynamics of suspended sediment transport and yield in a large agricultural catchment, Southwest France, Earth Surface Processes and Landforms, 35, 1289-1301.

Ouyang, W., Huang, H.B., Hao, F.H., Shan, Y.S., Guo, B.B., 2012. Evaluating spatial interaction of soil property with non-point source pollution at watershed scale: The phosphorus indicator in Northeast China. Science of the Total Environment, 432, 412-421.

Ouyang, W., Skidmore, A.K., Toxopeus, A.G., Hao, F.H., 2010. Long-term vegetation landscape pattern with non point source nutrient pollution in upper stream of Yellow River basin. Journal of Hydrology, 389, 373-380.

Ouyang, W., Song, K.Y., Wang, X.L., Hao, F.H., 2014. Non-point source pollution dynamics under long-term agricultural development and relationship with landscape dynamics. Ecological Indicators, 45, 579-589.

Quinton, J.N., Catt, J.A., 2007. Enrichment of heavy metals in sediment resulting from soil erosion on agricultural fields. Environmental Science & Technology, 41, 3495-3500.

Rao, N.S., Easton, Z.M., Schneiderman, E.M., Zion, M.S., Lee, D.R., Steenhuis, T.S., 2009. Modeling watershed-scale effectiveness of agricultural best management practices to reduce phosphorus loading. Journal of Environmental Management, 90, 1385-1395.

San Miguel, E.G., Bolivar, J.P., Garcia-Tenorio, R., 2004. Vertical distribution of Th-isotope ratios, ^{210}Pb, ^{226}Ra and ^{137}Cs in sediment cores from an estuary affected by anthropogenic releases. Science of the Total Environment, 318, 143-157.

Saravana Kumara, U., Navada, S.V., Rao, S.M., Nachiappan, Rm.P., Kumar, Bhishm, Krishnamoorthy, T.M., Jha, S.K., Shukla, V.K., 1999. Determination of recent sedimentation rates and pattern in Lake Naini, India by ^{210}Pb and ^{137}Cs dating techniques. Applied Radiation and Isotopes, 51, 97-105.

Shotyk, W., 2002. The chronology of anthropogenic, atmospheric Pb deposition recorded by peat cores in three minerogenic peat deposits from Switzerland. Science of the Total Environment, 292, 19-31.

Tang, W.Z., Shan, B.Q., Zhang, H., Mao, Z.P., 2010. Heavy metal sources and associated risk in response to

agricultural intensification in the estuarine sediments of Chaohu Lake Valley, East China. Journal of Hazardous Materials, 176, 945-951.
Tesoriero, A.J., Duff, J.H., Wolock, D.M., Spahr, N.E., Almendinger, J.E., 2009. Identifying pathways and processes affecting nitrate and orthophosphate inputs to streams in agricultural watersheds. Journal of Environmental Quality, 38, 1892-1900.
Wang, G.P., Liu, J.S., Tang, J., 2004. The long-term nutrient accumulation with respect to anthropogenic impacts in the sediments from two freshwater marshes (Xianghai Wetlands, Northeast China). Water Research, 38, 4462-4474.
Xia, P., Meng, X.W., Yin, P., Cao, Z.M., Wang, X.Q., 2011. Eighty-year sedimentary record of heavy metal inputs in the intertidal sediments from the Nanliu River estuary, Beibu Gulf of South China Sea. Environmental Pollution, 159, 92-99.
Yang, Y.G., He, Z.L., Wang, Y.B., Fan, J.H., Liang, Z.B., Stoffella, P.J., 2013. Dissolved organic matter in relation to nutrients (N and P) and heavy metals in surface runoff water as affected by temporal variation and land uses-A case study from Indian River Area, south Florida, USA. Agricultural Water Management, 118, 38-49.
Zia, H., Harris, N.R., Merrett, G.V., Rivers, M., Coles, N., 2013. The impact of agricultural activities on water quality: A case for collaborative catchment-scale management using integrated wireless sensor networks. Computers and Electronics in Agriculture, 96, 126-138.
Ouyang, W., Liu, B., Huang, H.B., Hao, F.H., 2015. Watershed water circle dynamics during long term farmland conversion in freeze-thawing area. Journal of Hydrology, 523, 555-562.
Ouyang, W., Huang, H.B., Hao, F.H., Guo, B.B., 2013. Synergistic impacts of land-use change and soil property variation on non-point source nitrogen pollution in a freeze-thaw area. Journal of Hydrology, 495(12), 126-134.
Ramalhosa, E., Segade, SR., Pereira, E., Vale, C., Duarte, A., 2006. Mercury cycling between the water column and surface sediments in a contaminated area. Water Research, 40(15), 2893-2900.
Shen, Z.Y., Zhong, Y.C., Huang, Q., Chen, L., 2015. Identifying non-point source priority management areas in watersheds with multiple functional zones. Water Research, 68(1): 563-571.
Smith, E., 2001. Pollutant concentrations of stormwater and captured sediment in flood control sumps draining an urban watershed. Water Research, 35(13), 3117-3126.
Álvarez-Iglesias, P., Quintana, B., Rubio, B., Pérez-Arlucea, M., 2007. Sedimentation rates and trace metal input history in intertidal sediments from San Simón Bay (Ría de Vigo, NW Spain) derived from 210Pb and 137Cs chronology. Journal of Environmental Radioactivity, 98(3), 229-250.

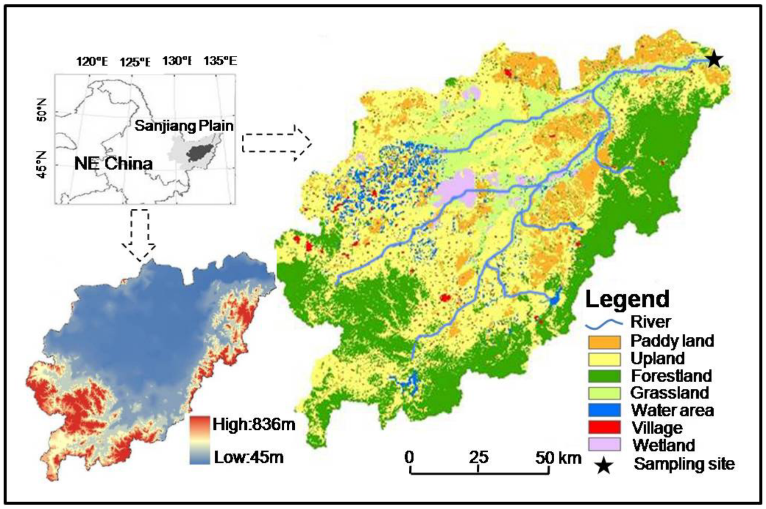

Fig.1 Location of the study area showing topography, land uses and sampling site

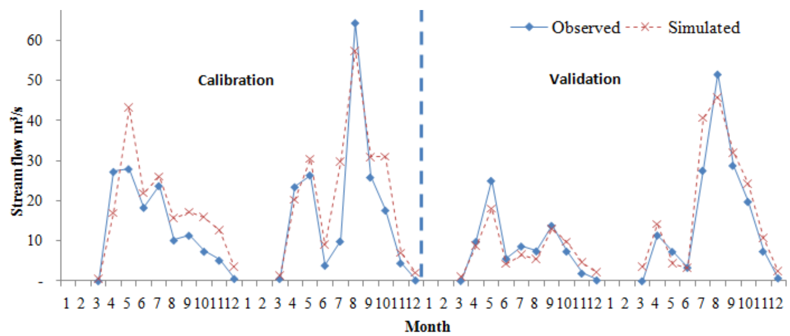

Fig. 2 Calibration and validation of the streamflow

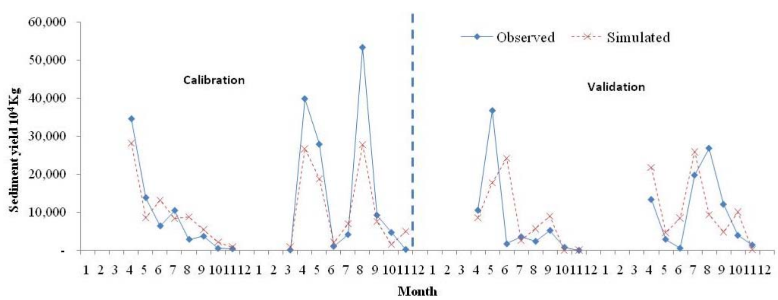

Fig. 3 Calibration and validation of the sand concentration

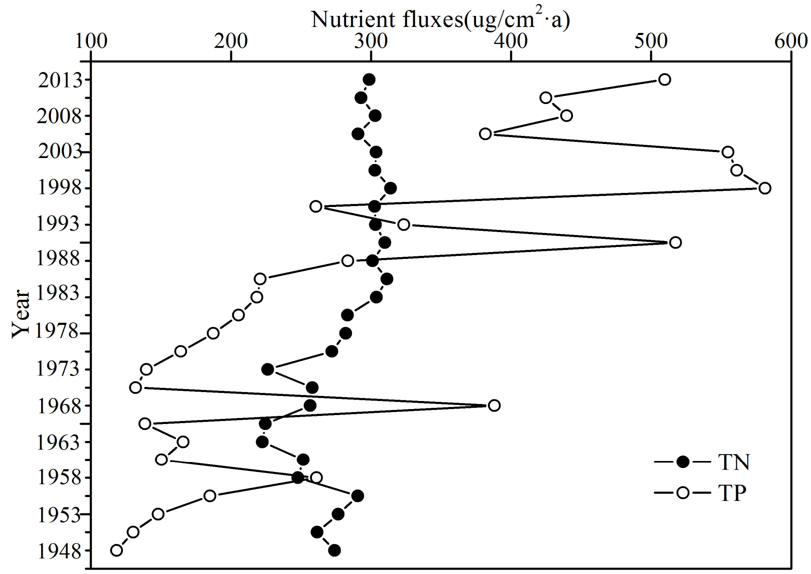

Fig. 4 Historical accumulation of total nitrogen and phosphorus in the sediment core

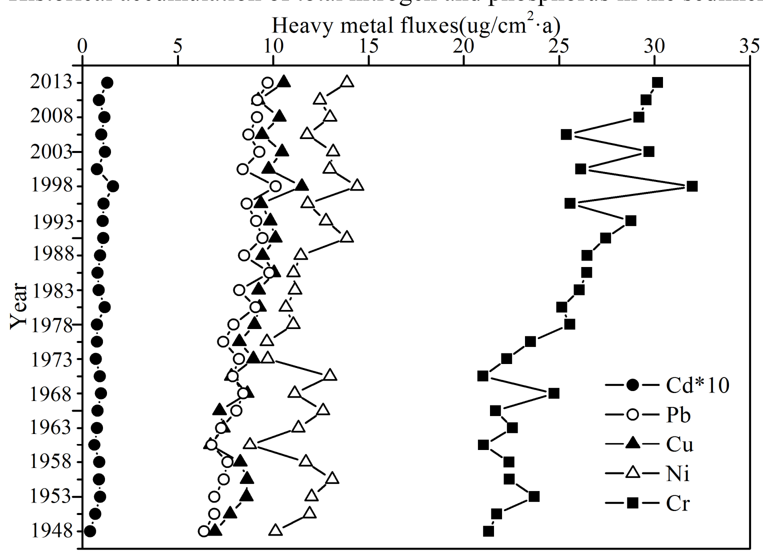

Fig. 5 Historical accumulation of heavy metals in the sediment core

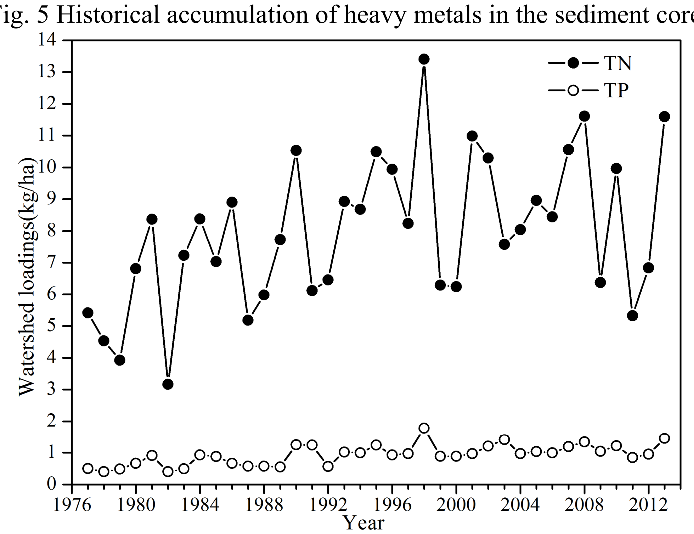

Fig. 6 Long-term watershed NPS total nitrogen and phosphorus loadings

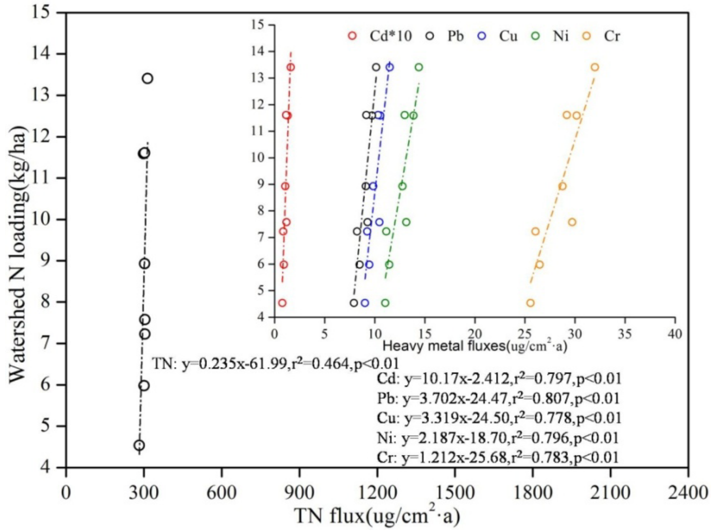

Fig. 7 Relationships between watershed NPS total nitrogen loading and sediment properties

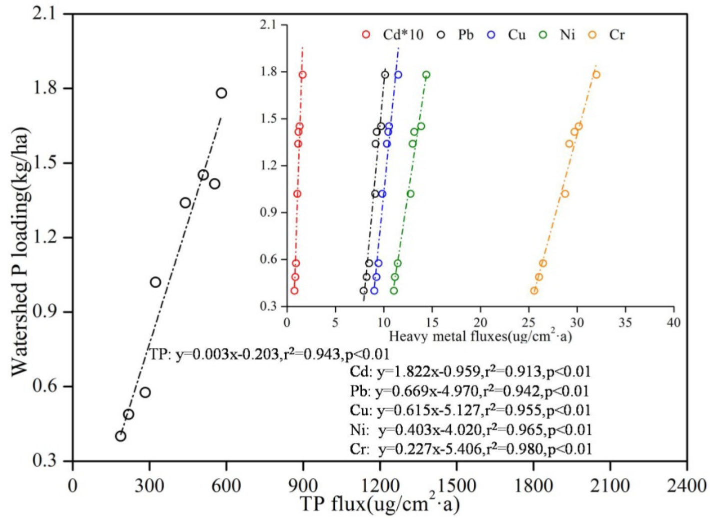

Fig. 8 Relationships between watershed NPS total phosphorus loading and sediment properties

Table 1 Total, supported and excess ^{210}Pb activities, as well as CRS modeled sedimentation rates

Depth (cm)	$^{210}Pb_{tot}$ (Bg/kg)	$^{210}Pb_{sup}$ (Bg/kg)	$^{210}Pb_{ex}$ (Bg/kg)	Mass rate (mg/cm^2·a)	Linear rate (cm/a)	Sedimentation date (Year)
0-1	28.56	14.37	14.19	497.71	0.62	2013
1-2	28.64	14.89	13.75	488.18	0.60	
2-3	27.34	14.75	12.59	504.82	0.60	2008
3-4	26.38	13.95	12.43	484.76	0.55	
4-5	27.49	16.25	11.24	506.16	0.60	2003
5-6	25.68	15.01	10.67	504.71	0.58	
6-7	24.17	14.42	9.75	523.15	0.59	1998
7-8	24.30	14.72	9.58	504.16	0.59	
8-9	23.59	14.54	9.05	505.47	0.60	1993
9-10	21.70	13.31	8.39	516.41	0.61	
10-11	24.02	15.82	8.20	501.66	0.58	1988
11-12	21.21	13.69	7.52	519.00	0.61	
12-13	22.69	15.40	7.29	506.34	0.57	1983
13-14	21.52	14.12	7.40	472.15	0.53	
14-15	21.03	14.02	7.01	469.77	0.53	1978
15-16	23.21	16.43	6.78	453.36	0.48	
16-17	22.02	15.61	6.41	452.50	0.49	1973
17-18	22.71	16.41	6.30	430.03	0.45	
18-19	19.68	13.79	5.89	427.52	0.44	1968
19-20	20.29	15.11	5.18	449.13	0.47	
20-21	21.91	16.97	4.94	444.86	0.46	1963
21-22	21.04	16.13	4.91	419.44	0.42	
22-23	19.39	14.80	4.59	412.94	0.41	1958
23-24	20.50	16.31	4.19	415.20	0.42	
24-25	18.90	14.80	4.10	394.95	0.39	1953
25-26	20.12	16.11	4.01	373.68	0.36	
26-27	20.28	16.31	3.97	342.54	0.32	1948
27-28	18.58	14.78	3.80	319.59	0.31	
28-29	18.56	15.25	3.31	330.27	0.32	1943
29-30	18.97	15.56	3.41	293.08	0.26	
30-31	18.50	15.61	2.89	300.66	0.27	1938
31-32	19.00	16.21	2.79	278.04	0.25	
32-33	18.20	15.52	2.68	253.73	0.22	1933
33-34	19.18	16.68	2.50	236.66	0.20	
34-35	18.51	16.00	2.51	199.30	0.17	1928
35-36	18.80	16.58	2.22	184.01	0.16	
36-37	17.83	15.92	1.91	163.04	0.12	1923
37-38	16.97	14.97	2.00	124.56	0.09	
38-39	17.52	15.68	1.84	89.70	0.06	1918
39-40	17.43	15.62	1.81	45.86	0.04	